

A constitutive model for fiber-reinforced extrudable fresh cementitious paste

Xiangming Zhou*¹ and Zongjin Li²

¹*School of Engineering and Design, Brunel University, Uxbridge, Middlesex UB8 3PH, United Kingdom*

²*Department of Civil and Environmental Engineering, The Hong Kong University of Science and Technology, Clear Water Bay, Kowloon, Hong Kong*

(Received October 22, 2009, Accepted August 18, 2010)

Abstract. In this paper, time-continuous constitutive equations for strain rate-dependent materials are presented first, among which those for the overstress and the consistency viscoplastic models are considered. By allowing the stress states to be outside the yield surface, the overstress viscoplastic model directly defines the flow rule for viscoplastic strain rate. In comparison, a rate-dependent yield surface is defined in the consistency viscoplastic model, so that the standard Kuhn-Tucker loading/unloading condition still remains true for rate-dependent plasticity. Based on the formulation of the consistency viscoplasticity, a computational elasto-viscoplastic constitutive model is proposed for the short fiber-reinforced fresh cementitious paste for extrusion purpose. The proposed constitutive model adopts the von-Mises yield criterion, the associated flow rule and nonlinear strain rate-hardening law. It is found that the predicted flow stresses of the extrudable fresh cementitious paste agree well with experimental results. The rate-form constitutive equations are then integrated into an incremental formulation, which is implemented into a numerical framework based on ANSYS/LS-DYNA finite element code. Then, a series of upsetting and ram extrusion processes are simulated. It is found that the predicted forming load-time data are in good agreement with experimental results, suggesting that the proposed constitutive model could describe the elasto-viscoplastic behavior of the short fiber-reinforced extrudable fresh cementitious paste.

Keywords: viscoplastic; cement paste; extrusion; rheology; flow stress; constitutive modeling.

1. Introduction

Extrusion is a material processing method for manufacturing semi-solid paste-like products widely used in mechanical, chemical, ceramic, food and pharmaceutical industries. It has been introduced into concrete industry, as an economical, efficient and environmental-friendly material processing technology, for only around 15 years for manufacturing building and construction products (Shao *et al.* 1995, Shao and Shah 1997, Aldea *et al.* 1998, Li *et al.* 1999, Li *et al.* 2001, Peled and Shah 2003, Li *et al.* 2004, Kuder and Shah 2007a, Shen *et al.* 2008). It has been found that short fibers can be aligned along extrusion direction (Qian *et al.* 2003), and the extrusion technique can largely improve mechanical performance of cement composites (Li *et al.* 2001, Peled and Shah 2003). Though lot of extrusion practice has been successfully achieved on cement-based materials, very limited research has been carried out on constitutive behavior of extrudable fresh cementitious paste and the

* Corresponding author, Lecturer, E-mail: Xiangming.Zhou@brunel.ac.uk

extrusion process itself. It should be noted that the behavior of extrudable fresh cementitious pastes is largely different from that of traditional cement paste, mortar, suspension, slurry, fresh self-compacting concrete or other fresh concrete which normally have larger water-to-binder ratio and exhibit more fluidity. These materials are normally modeled as Newtonian or Bingham fluids. Short fiber-reinforced fresh cementitious pastes for extrusion purpose are dough-like materials with rheology enhancing admixture, which exhibit almost no fluidity, but high cohesion and pseudo-plastic behavior (Srinivasan *et al.* 1999). They are somehow more like clay rather than traditional cement pastes. So far, there is very limited quantitative data available for describing behavior of extrudable fresh cementitious paste. Ram rheometry was adopted for characterizing rheology behavior of extrudable fresh cementitious pastes (Srinivasan *et al.* 1999, Zhou and Li 2005a). The extrusion behavior of these highly condensed cementitious pastes was described in terms of the relationship between extrusion pressure and paste flow velocity using a physically phenomenal model. Capillary rheometry was adopted to calibrate the post-yield steady-state shear flow behavior of fresh cementitious paste for extrusion purpose (Zhou and Li 2005b, Alfani *et al.* 2007, Kuder and Shah 2007b). It has been found that the shear flow behavior of extrudable fresh cementitious paste can be described by the Herschel-Bulkley model (Zhou and Li 2005b). Squeezing test was utilized as a rheological behavior identification tool for firm cement-based materials to evaluate their extrusion ability (Toutou *et al.* 2005). It was concluded that extrudability requires a balance between processing and material rheological properties. Upsetting test is the uniaxial compression of a cylindrical specimen between flat platens, which was employed to derive the quantitative relationship between flow stress and true strain, of fresh cementitious paste for extrusion purpose, under a series of true strain rates by Zhou and Li (2006). It was found that the strain rate-hardening effect dominates the constitutive behavior of extrudable fresh cementitious paste. Theoretical solution of squeezing flow for the fresh cementitious paste for extrusion purpose was presented by Li and Li (2007). They pointed out that the constitutive behavior of the fresh cementitious paste for extrusion purpose is mainly governed by rheological (strain rate-dependent) effect while plastic (strain-dependent) effect is not significant, especially when the fresh cementitious paste exhibits large strain.

In numerical simulation of material forming processes, such as extrusion and upsetting, one particular challenge is to model the complex constitutive material behavior. Normally, a complete description of constitutive behavior of a material in a forming process involves stress-strain response as a function of not only large strain, but also large strain rate, varying stress state, history of loading, etc. Perzyna (1966) underlined the fact that the application of the theory of plasticity, in which rheological effect is disregarded, leads to large discrepancies between theoretical and experimental results for rate-dependent materials. However, it is difficult to introduce both rheological and plastic effects simultaneously into a material constitutive model. For instance, as a result of viscous effect, a material's current states of stress and strain are time-dependent. Plastic effect, on the other hand, make these states depend on the loading path or history. Thus the simultaneous introduction of viscous and plastic effects, into a material constitutive model, results in the material behavior depending on both time and loading history. One way to circumvent this problem is to adopt constitutive laws relating the flow stress to the deformation history by means of rate-dependent internal state variables (Santhanam 2000, Al-Haik *et al.* 2001). On the other hand, in numerical simulation of extrusion of polymers, hot metals and super-alloys, it is common to use viscoplastic constitutive models and neglect elastic deformation of materials (Kobayashi *et al.* 1989). The reason for this is that elastic deformations are normally small compared to plastic deformations during a material forming process. However, this is not always true. In some areas of an extrusion process,

elastic deformations are dominant and cannot be neglected (Lof 2001). For example, the deformation of the fresh cementitious paste, in the barrel during ram extrusion, is very small and the elastic effect is dominant, so that a viscoplastic constitutive model may not be appropriate for describing its behavior. It has been found that, by adopting a viscoplastic constitutive model for the extrudable fresh cementitious paste, there was large discrepancy in flow stress between experimental and theoretical results (Li and Li 2007). This discrepancy was ascribed to neglect the elastic response of the fresh cementitious paste. One approach, to take into account material's elasticity, is to introduce an elastic domain in the viscoplastic constitutive model, and let the inelastic strain rate depend only on the stress outside this domain, resulting in the so-called overstress viscoplastic model (Chaboche 1989).

In this paper, time-continuous constitutive equations for rate-dependent materials are presented first. A rate-form elasto-viscoplastic constitutive model is then proposed for the short fiber-reinforced fresh cementitious paste for extrusion purpose, within the framework of continuum mechanics and based on the von Mises yield criterion, the associated flow rule and nonlinear isotropic strain rate-hardening law. For each of the physical phenomena included in the model, one or more material constants are required. However, all these constants can be obtained from material tests and simple mathematical procedures without the need of numerical methods. Identification of these material constants for the short fiber-reinforced extrudable fresh cementitious paste is then demonstrated based on experimental results. The flow stresses of the paste in upsetting tests, predicted by the proposed constitutive model, are compared with experimental results. The rate-form constitutive equations are then integrated into an incremental formulation, which is implemented into a numerical procedure based on ANSYS/LS-DYNA explicit finite element code. Finally, various forming processes of the short fiber-reinforced fresh cementitious paste, including upsetting and ram extrusion, are simulated. The forming load-time data, obtained from numerical simulation, are compared with experimental results to test the applicability of the proposed constitutive model for the short fiber-reinforced fresh cementitious paste for extrusion purpose.

2. Elasto-viscoplastic constitutive models for strain rate-dependent materials

2.1 Time continuous constitutive equations

A time-continuous model normally forms the basis for the constitutive equations in numerical simulation of elasto-viscoplastic material behavior. In such a model, the relation between stress and strain, in both the elastic and the plastic domains, is usually defined in a rate form. Based on the infinitesimal deformation theory, it is reasonable to assume that the rate of deformation can be additively decomposed into an elastic (reversible) part and an inelastic (irreversible) part. For simplicity, only isotropic material behavior is considered here. It is further assumed that isotropic strain rate-hardening law is sufficient to describe the evolution of the yield surface during plastic deformation of the short fiber-reinforced highly condensed fresh cementitious paste. The strain rate-hardening law is described in terms of the accumulated equivalent viscoplastic strain rate, $\dot{\varepsilon}^{\bar{v}p}$. Assuming a J_2 plastic flow, the von Mises criterion is used to define the equivalent flow stress, $\bar{\sigma}$. Thus, the time-continuous elasto-viscoplastic model for a rate-dependent material can be described by a set of constitutive equations presented in a rate form as

$$\dot{\varepsilon} = \dot{\varepsilon}^e + \dot{\varepsilon}^{vp} \quad (1)$$

$$\dot{\sigma} = C:(\dot{\varepsilon} - \dot{\varepsilon}^{vp}) \quad (2)$$

$$\dot{\varepsilon}^{vp} = \dot{\Lambda} S \quad (3)$$

$$g(\sigma, \varepsilon^{\bar{vp}}, \dot{\varepsilon}^{\bar{vp}}) = \bar{\sigma} - \sigma_f(\varepsilon^{\bar{vp}}, \dot{\varepsilon}^{\bar{vp}}) \quad (4)$$

$$\dot{\Lambda} \geq 0, \dot{\Lambda} g = 0, g \leq 0 \quad (5)$$

Eq. (1) is the rate form of strain tensor decomposition. Here, the total strain tensor, ε , is assumed to be the sum of an elastic part, ε^e , and a viscoplastic part, ε^{vp} , as is the total strain rate, $\dot{\varepsilon}$.

Eq. (2) is the linear elastic relation between the Cauchy stress tensor, σ , and the elastic strain tensor, $\varepsilon^e = \varepsilon - \varepsilon^{vp}$, in the rate form. Based on the assumption of isotropic material behavior, the elastic constant, C , is a tensor whose individual components can be calculated from values of Young's modulus, E , and the Poisson's ratio, ν . The symbol $(:)$ represents the doubly contracted tensor product. The extension of Eq. (2) can be formulated as

$$\dot{\sigma}_{ij} = C_{ijkl}(\dot{\varepsilon}_{kl} - \dot{\varepsilon}_{kl}^{vp}) \quad (6)$$

where

$$C_{ijkl} = \mu(\delta_{ik}\delta_{jl} + \delta_{il}\delta_{jk}) + \lambda\delta_{ij}\delta_{kl} \quad (7)$$

In Eq. (7), μ and λ are the Lamé constants, δ_{ij} denotes Kronecker's delta and μ is actually the shear modulus of the material.

Eq. (3) is the flow rule for viscoplastic strain rate. Here the concept of the associate flow rule in rate-independent plasticity is extended to viscoplasticity. Based on this flow rule, the viscoplastic strain rate is in the direction of the deviatoric stress tensor, S , which is defined by

$$S = \sigma - \frac{1}{3}tr(\sigma)I \quad (8)$$

The viscoplastic multiplier, $\dot{\Lambda}$, in Eq. (3) is used to scale the viscoplastic strain rate.

The specific constitutive behavior of the material is given by $\sigma_f = \sigma_f(\varepsilon^{\bar{vp}}, \dot{\varepsilon}^{\bar{vp}})$ in Eq. (4) as a relation between the equivalent flow stress and the internal state variables, $\varepsilon^{\bar{vp}}$ and $\dot{\varepsilon}^{\bar{vp}}$, which represent the equivalent viscoplastic strain and the equivalent viscoplastic strain rate, respectively, and are defined as

$$\varepsilon^{\bar{vp}} = \sqrt{\frac{2}{3} \varepsilon^{vp} : \varepsilon^{vp}} \quad (9)$$

and

$$\dot{\varepsilon}^{\bar{vp}} = \sqrt{\frac{2}{3} \dot{\varepsilon}^{vp} : \dot{\varepsilon}^{vp}} \quad (10)$$

Eq. (4) actually gives the limit function, which describes the rate dependent behavior of the material in plastic domain. It can also be interpreted as a generalization of the yield function from rate-independent to rate-dependent materials. The equivalent flow stress is calculated according to the von Mises yield criterion as

$$\bar{\sigma} = \sqrt{3J_2} = \sqrt{\frac{3}{2}S:S} \quad (11)$$

Eq. (5) is the standard Kuhn-Tucker loading/unloading condition (Simo and Hughes 1998). The material can be in either of two states; the elastic state, in which the viscoplastic multiplier, $\dot{\Lambda}$, is equal to zero and the limit function, g , is lower or equal to zero, and the plastic state, in which the viscoplastic multiplier is larger than zero and the limit function is equal to zero. At the boundary between these two states, the viscoplastic strain rate and the limit function are both equal to zero and the limit function corresponds to the yield function in rate-independent plasticity.

2.2 The limit function and the flow rule for viscoplastic strain rate

In the case of rate-independent plasticity, the equivalent plastic strain rate is removed from the material's flow stress constitutive equation, $\bar{\sigma}_f = \sigma_f(\bar{\varepsilon}^p, \dot{\varepsilon}^p)$, resulting in $\bar{\sigma}_f = \sigma_f(\bar{\varepsilon}^p)$. In classical plasticity theory, a yield function, $f = f(\sigma, \sigma_f(\bar{\varepsilon}^p))$, is normally given and, in such a case, the limit function, $g = g(\sigma, \bar{\varepsilon}^p)$ in Eq. (4), is equal to the yield function. The admissible stress states are constrained to remain on or within the elastic domain, i.e. $f \leq 0$ or $g \leq 0$. The notion of irreversibility, linked to the plastic part, is built into the formulation by introducing equations of evolution for $\bar{\varepsilon}^p$ (flow rule) and $\sigma_f(\bar{\varepsilon}^p)$ (hardening laws). The plastic multiplier, $\dot{\Lambda}$, which is sometimes called the consistency parameter as well, can be determined by expressing the so-called consistency condition.

However, the fundamental difference between plasticity and viscoplasticity is that, in plasticity, there is a unique unloading state associated with each state of homogeneous deformation. This is not the case for viscoplasticity, since the unloading behavior of a viscoplastic material also depends on the unloading rate. Thus, in rate-dependent plasticity, the consistency parameter, $\dot{\Lambda}$, cannot be determined simply by expressing the consistency condition only (Ponthot 2002). One more equation is needed. Various such equations have been proposed to express the consistency parameter, $\dot{\Lambda}$, in terms of the current stress. Most of these formulations are introduced by so-called overstress viscoplastic models, for instance, the Perzyna model (Simo and Hughes 1998). Contrary to the case of rate-independent plasticity, the equivalent flow stress, $\bar{\sigma}$, is no longer constrained to remain less than or equal to the yield stress in an overstress viscoplastic model, but it can be allowed out of the yield surface, i.e. $\bar{\sigma} \geq \sigma_y$. The part of the stress that is outside the yield surface, i.e. $H = \langle \bar{\sigma} - \sigma_y \rangle$ where $\langle x \rangle = x$ if $x \geq 0$ and $\langle x \rangle = 0$ if $x < 0$, is called the overstress, which determines the viscoplastic strain rate, $\dot{\varepsilon}^{vp}$. Obviously, a viscoplastic deformation can take place only if the overstress, H , is positive and, in such a case, the yield function is larger than zero, i.e. $f > 0$. For example, the classical Perzyna overstress viscoplastic model could be considered as a penalized regularization of rate-independent plasticity, where the viscoplastic multiplier, $\dot{\Lambda}$, is defined by

$$\dot{\Lambda} = \gamma \langle \phi(f) \rangle \quad (12)$$

in which γ is a viscosity parameter, and $\phi(f)$ is an arbitrary function of the yield surface. A power law is often chosen for the overstress function, $\phi(f)$, as

$$\phi(f) = \left(\frac{f}{\sigma_y(\bar{\varepsilon}^{vp})} \right)^j = \left(\frac{\bar{\sigma} - \sigma_y(\bar{\varepsilon}^{vp})}{\sigma_y(\bar{\varepsilon}^{vp})} \right)^j \quad (13)$$

where j is a rate sensitivity parameter of the material.

2.3 Strain rate-dependent yield function

An important distinction of the overstress viscoplastic models, from the classical rate-independent plasticity models, is noted in that the current stress states can be outside the yield surface, i.e. the yield function may have a value larger than zero. Therefore, the standard Kuhn-Tucker loading/unloading condition is violated (Simo and Hughes 1998). To solve this problem and make the rate-dependent plasticity consistent with the rate-independent plasticity, a “yield” function that is strain rate-dependent is normally defined to introduce viscoplasticity. Thus, the strain rate contribution can be explicitly built into the constitutive model through this rate-dependent yield function (Wang *et al.* 1997, Lof and Boogaard 2001, Ponthot 2002). The rate-dependent yield function is denoted by $\bar{f} = \bar{f}(\sigma, \sigma_y)$ in order to differ from the conventional rate-independent yield function, $f = f(\sigma, \sigma_y)$. This rate-dependent “yield” function may vary with the internal state variables representing the loading history, such as the (equivalent) plastic strain and/or the (equivalent) plastic strain rate. It will be shown later that, by adopting such a rate-dependent yield function, the incremental formulation of rate-dependent plasticity is similar to that of rate-independent plasticity. Thus the Kuhn-Tucker loading/unloading condition still remains true for rate-dependent plasticity. Therefore, this kind of viscoplastic model is named as the consistency model. This approach is adopted in this paper for the short fiber-reinforced fresh cementitious paste for extrusion purpose, where the relation among stress, strain and strain rate is directly given by the limit function, which can be interpreted as a rate-dependent yield function and states that, in plastic domain, the equivalent stress, $\bar{\sigma}$, must be equal to the flow stress, σ_f ,

$$g(\sigma, \varepsilon^{\bar{v}p}, \dot{\varepsilon}^{\bar{v}p}) = \bar{\sigma} - \sigma_f(\varepsilon^{\bar{v}p}, \dot{\varepsilon}^{\bar{v}p}) = 0 \quad (14)$$

In fact, the Perzyna overstress viscoplastic model can be included by the consistency model after changing its form and introducing a rate-dependent yield function described as below. In classical Perzyna overstress viscoplastic model, the plastic part of the strain rate is given by

$$\dot{\varepsilon}^{\bar{v}p} = \dot{\lambda} \frac{\partial f}{\partial \sigma} = \dot{\lambda} N \quad (15)$$

where N is the direction of the viscoplastic strain rate. It is defined as the gradient of the flow surface in stress space following associated flow rule and $N:N = 3/2$. In such a case, the equivalent viscoplastic strain rate is given by

$$\dot{\varepsilon}^{\bar{v}p} = \sqrt{\frac{2}{3} \dot{\varepsilon}^{\bar{v}p} : \dot{\varepsilon}^{\bar{v}p}} = \sqrt{\frac{2}{3} \gamma \phi(f) N : \gamma \phi(f) N} = \sqrt{\frac{2}{3} N : N |\gamma \phi(f)|} = \gamma \left(\frac{\bar{\sigma} - \sigma_y(\varepsilon^{\bar{v}p})}{\sigma_y(\varepsilon^{\bar{v}p})} \right)^j \quad (16)$$

Rearranging Eq. (16) yields

$$\bar{\sigma} - \sigma_y(\varepsilon^{\bar{v}p}) - \sigma_y(\varepsilon^{\bar{v}p}) \left(\frac{\dot{\varepsilon}^{\bar{v}p}}{\gamma} \right)^{1/j} = 0 \quad (17)$$

So that, in the viscoplastic domain, a new constraint (yield criterion) can be defined as

$$\bar{f} = \bar{\sigma} - \sigma_y(\varepsilon^{\bar{v}p}) - \sigma_y(\varepsilon^{\bar{v}p}) \left(\frac{\dot{\varepsilon}^{\bar{v}p}}{\gamma} \right)^{1/j} = 0 \quad (18)$$

Eq. (18) is a generalization of the classical von Mises yield criterion for rate-dependent material

and can be considered as the rate-dependent yield function. From this point of view, the classical Perzyna overstress viscoplastic model can also be classified as one kind of consistency viscoplastic models. In the elastic domain, both f and \bar{f} are equivalent since, in that case

$$\dot{\varepsilon}^{\bar{y}p} = 0 \text{ and } \bar{\sigma} \leq \sigma_y(\varepsilon^{\bar{y}p}) \tag{19}$$

so that, similar to the rate-independent plasticity

$$\bar{f} \leq 0 \tag{20}$$

The extended criterion (Eq. (18)) allows a generalization of the Kuhn-Tucker condition which, for viscoplastic material, can be extended to the following form

$$\dot{\Lambda} > 0, \dot{\Lambda}\bar{f} = 0, \bar{f} \leq 0 \tag{21}$$

2.4 Stress update algorithm in a computational formulation

The rate-form constitutive equations (Eqs. (1-5)) can not be directly implemented into a numerical framework so that it becomes necessary to integrate them to obtain an incremental formulation. To do it, the viscoplastic flow rule (Eq. (3)) has to be integrated over the time interval $[t_n, t_{n+1}]$. Here the starting point is from time t , with the known converged state, $[\varepsilon_t, \varepsilon_t^{yp}, \sigma_t, \varepsilon_t^{\bar{y}p}]$, to predict the unknown state at time $t + \Delta t$, $[\varepsilon_{t+\Delta t}, \varepsilon_{t+\Delta t}^{yp}, \sigma_{t+\Delta t}, \varepsilon_{t+\Delta t}^{\bar{y}p}]$, with a prescribed incremental nodal displacement defining the geometric update during the numerical process. To integrate these equations in time domain, the general elastic-predictor/plastic-predictor methodology (return mapping algorithm) (Simo and Hughes 1998, Belytschko *et al.* 2000) for time-independent elasticity and plasticity is adopted, but here the methodology is extended to the time-dependent elasticity and plasticity. In general, the problem is solved sequentially by first solving the elastic problem for the strain increment, while keeping the irreversible strain frozen, which produces a trial elastic stress, σ_{tr} . If the trial stress is inside the yield surface, i.e. $f(\sigma_{tr}, \sigma_y) \leq 0$ (see Fig. 1), and satisfies the Kuhn-Tucker loading/unloading condition, the process is clearly elastic and the trial stress is in fact the true stress. On the other hand, if the trial stress is outside the yield surface, i.e. $f(\sigma_{tr}, \sigma_y) > 0$ (see Fig. 1), which, in turn, implies $\bar{f} > 0$, the Kuhn-Tucker loading/unloading condition is violated. The trial stress now lies outside the yield surface and the material is in the plastic domain. The trial stress is then taken

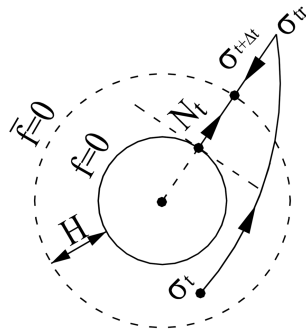


Fig. 1 Conceptual representation of the elastic/viscoplastic corrector algorithm (according to the Euler backward (radial return) integration)

as the initial condition for the solution of the viscoplastic corrector problem, and the predictor step is thus followed by a viscoplastic correction. The objective of this second step is to restore consistency by returning the trial stress back to the rate-dependent yield surface, \bar{f} (see Fig. 1). This stress update procedure is demonstrated graphically in Fig. 1. In an incremental process, the incremental strain tensor, $\Delta\varepsilon$, is decomposed into an elastic part, $\Delta\varepsilon^e$, and a viscoplastic part, $\Delta\varepsilon^{vp}$, according to

$$\Delta\varepsilon = \Delta\varepsilon^e + \Delta\varepsilon^{vp} \quad (22)$$

The incremental stress is related to the elastic response by

$$\Delta\sigma = C(\Delta\varepsilon - \Delta\varepsilon^{vp}) \quad (23)$$

Therefore, the key feature of stress updates is characterized by estimating the incremental viscoplastic strain $\Delta\varepsilon^{vp}$. In this study, a generalized trapezoidal rule is adopted to approximate the viscoplastic flow, resulting in

$$\Delta\varepsilon^{vp} = \int_{t_n}^{t_{n+1}} \dot{\Lambda} \frac{\partial Q}{\partial \sigma} dt \approx \Delta\Lambda \left((1-\alpha) \left[\frac{\partial Q}{\partial \sigma} \right]_n + \alpha \left[\frac{\partial Q}{\partial \sigma} \right]_{n+1} \right) \quad (24)$$

Generalizing the notion of associated plasticity to viscoplasticity for J_2 flow, the viscoplastic potential, Q , coincides with the rate-dependent yield function, \bar{f} . Differentiating g with respect to the stress, σ , yields the result that the direction of the plastic strain is in the direction of the deviatoric stress tensor, S . Thus, the trapezoidal algorithm yields

$$\Delta\varepsilon^{vp} = \Delta\Lambda((1-\alpha)S_n + \alpha S_{n+1}) = \Delta\Lambda S^* \quad (25)$$

where the updated deviatoric stress tensor, S^* , is introduced to denote the direction of the plastic strain during the increment and α is an interpolation parameter, such that $0 \leq \alpha \leq 1$. Accordingly, the incremental equivalent viscoplastic strain rate is defined by

$$\Delta\varepsilon^{\bar{vp}} = \sqrt{\frac{2}{3}} \Delta\varepsilon^{vp} : \Delta\varepsilon^{vp} = \Delta\Lambda \sqrt{\frac{2}{3}} S^* : S^* \quad (26)$$

The values of state variables $\varepsilon_{n+1}^{\bar{vp}}$ and $\dot{\varepsilon}_{n+1}^{\bar{vp}}$ at the end of the time increment are derived to be

$$\varepsilon_{n+1}^{\bar{vp}} = \varepsilon_n^{\bar{vp}} + \Delta\varepsilon^{\bar{vp}} \quad (27)$$

$$\dot{\varepsilon}_{n+1}^{\bar{vp}} = \frac{\Delta\varepsilon^{\bar{vp}}}{\Delta t} \quad (28)$$

The other two rate-form constitutive equations, Eqs. (4) and (5), can also be transformed into their corresponding incremental formulations as

$$g_{n+1} = \bar{\sigma}_{n+1} - \sigma_f(\varepsilon_{n+1}^{\bar{vp}}, \dot{\varepsilon}_{n+1}^{\bar{vp}}) = \sqrt{\frac{3}{2}} S_{n+1} : S_{n+1} - \sigma_f(\varepsilon_{n+1}^{\bar{vp}}, \dot{\varepsilon}_{n+1}^{\bar{vp}}) \quad (29)$$

and

$$\Delta\Lambda \geq 0, \Delta\Lambda g_{n+1} = 0, g_{n+1} \leq 0 \quad (30)$$

From the above equations, it becomes apparent that there is no fundamental difference in incremental formulations between rate-dependent and rate-independent plasticity. The equivalent plastic strain and/or equivalent plastic strain rate are calculated from the equivalent plastic strain increment. The

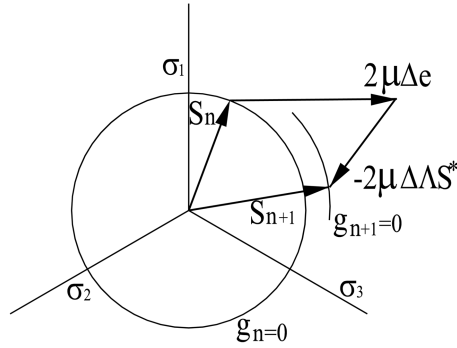


Fig. 2 Return mapping algorithm in the p-plane for stress updating

only difference is the introduction of the constant time increment, Δt , which introduces a time scale in the constitutive model for the rate-dependent plasticity.

The integration algorithm requires a function that relates the interpolation factor, α , to the increment of the plastic multiplier, $\Delta\Lambda$. Depending on the value of the interpolation factor, α , different return mapping algorithms are obtained. Taking $\alpha = 1/2$ coincides with the trapezoidal rule (mean normal), and $\alpha = 1$ results in Euler backward integration (radial return). For J_2 material flow, the generalized trapezoidal rule is unconditionally stable when $\alpha \geq 1/2$ (Ortiz and Popov 1985). Thus, the Euler backward (radial return) integration algorithm, with $\alpha = 1$, is adopted here, resulting in an explicit integration algorithm as

$$\Delta \varepsilon^{vp} = \Delta \Lambda \alpha S_{n+1} = \Delta \Lambda S_{n+1} \quad (31)$$

The deviatoric part of stress can be written as

$$S_{n+1} = S_n + 2\mu(\Delta e - \Delta \Lambda S^*) \quad (32)$$

as well as by enforcing Eq. (29). The return mapping algorithm of the deviatoric stress update in the π -plane is schematically shown in Fig. 2. In Eq. (32), Δe is the deviatoric part of the total strain increment. After substituting Eq. (32), together with the definitions of the state variables (Eqs. (26)-(28)), into Eq. (29), a scalar equation for $\Delta\Lambda$ can be obtained.

3. The constitutive law for flow stress of extrudable fresh cementitious paste

The constitutive behavior of the short fiber-reinforced fresh cementitious paste for extrusion purpose in plastic domain can be represented by an expression for the flow stress, $\bar{\sigma} = \bar{\sigma}(\varepsilon^{vp}, \dot{\varepsilon}^{vp})$, which describes the relationship among the equivalent flow stress, the equivalent viscoplastic strain and the equivalent viscoplastic strain rate. Previous studies indicated that plastic effect is not significant for the short fiber-reinforced fresh cementitious paste for extrusion purpose, rather, strain rate-hardening effect dominates (Zhou and Li 2006, Li and Li 2007). Therefore the equivalent plastic strain is not explicitly built into the formulation of the flow stress. A shear-form Herschel-Bulkley constitutive equation was established based on results of orifice and capillary extrusion, which could reasonably describe the steady-state post-yield shear flow behavior of the short fiber-reinforced fresh cementitious paste (Zhou and Li 2005b). This constitutive equation is formulated

Table 1 Mix formulation of the short fiber-reinforced fresh cementitious paste

Cement	Slag	SS1*	SS2*	PVA**	Methocel*	ADVA*	W/B
0.5	0.5	0.2	0.125	2%	1%	0.375%	0.27

*Presented in weight ratio of the binder

**Presented in the volume ratio of the readily prepared fresh mixture

by the relationship between the shear flow stress, τ , and the viscoplastic shear strain rate, $\dot{\gamma}^{vp}$, as

$$\tau = \tau_0 + k_{sc} (\dot{\gamma}^{vp})^n \quad (33)$$

where τ_0 is the static shear yield stress, k_{sc} and n represent the shear flow consistency, and the shear flow index, respectively. Experiments were conducted on the short fiber-reinforced fresh cementitious paste, with the mix formulation shown in Table 1, at various strains and strain rates. The basic constitutive compositions for the composite include Type I OPC (Ordinary Portland Cement) and slag with the weight ratio of 1:1 as the cementitious binder (B); 6 mm-long PVA (Polyvinyl Alcohol) fiber with an average diameter of 14 μm , two types of silica sands (denoted as SS1 and SS2 with the nominal diameters of 300-600 μm and 90-150 μm , respectively) from David Ball Comp. Ltd with a weight ratio of 8:5 as aggregates, Methocel powder, produced by Dow Chemical Comp. Ltd, as the rheology enhancer and ADVA solution, made by W. R. Grace (HK) Ltd, as the superplasticiser. The water-to-binder weight ratio (W/B) is 0.27 while the silica sands-to-binder weight ratio is 0.325. The dosage of ADVA solid powder is 0.375% of the weight of the binder and the powder is incorporated into the composite in the form of an aqueous solution with a concentration of 30% by weight as supplied by the manufacturer. The amount of PVA fibers incorporated is 2% of the volume of the readily mixed composite. The chemical compositions of the cement and slag are shown in Table 2. Based on orifice and capillary extrusion test results, the associated material parameters in Eq. (33) were obtained as $\tau_0 = 2.15$ kPa, $k_{sc} = 4.17$ kPa.s^{*n*} and $n = 0.38$ for the extrudable fresh cementitious paste (Zhou and Li 2005b). The Young's modulus, E , was obtained from experimental results of upsetting tests (Zhou and Li 2006). Here, a constant Young's modulus, $E = 8$ kPa, and a constant Poisson's ratio, $\nu = 0.465$, representing a nearly incompressible material behavior, were adopted for the short fiber-reinforced fresh cementitious paste for extrusion purpose.

The shear-form constitutive equation (Eq. (33)) is transformed into its pertinent uniaxial-form counterpart as follows. The generalized uniaxial-form Herschel-Bulkley relationship can be written as

$$\sigma = \sigma_0 + k (\dot{\epsilon}^{vp})^m \quad (34)$$

where σ , σ_0 , k and m are the flow stress, the equivalent static yield flow stress, the uniaxial bulk flow consistency and the uniaxial bulk flow index, respectively. For a material that obeys the von Mises yield criterion, the uniaxial form of the Herschel-Bulkley relationship, Eq. (34), may be obtained from the graph of shear stress against shear strain rate by plotting $\tau = \sigma/\sqrt{3}$ as a function

Table 2 Chemical compositions of cement and slag (% in weight)

	CaO	SiO ₂	Al ₂ O ₃	Fe ₂ O ₃	MgO	SO ₃	K ₂ O	Na ₂ O	TiO ₂	f-Cao	LOI
Cement	63.12	20.83	6.28	2.47	1.16	2.04	0.61	0.25	0.21	0.44	
slag	39.50	28.48	12.56	1.56	7.40	8.48	0.44	0.20	0.44		0.50

of $\dot{\gamma}^{ip} = \sqrt{3}\dot{\varepsilon}^{ip}$. Substituting $\tau = \sigma/(\sqrt{3})$ and $\dot{\gamma}^{ip} = \sqrt{3}\dot{\varepsilon}^{ip}$ into Eq. (33) yields.

$$\sigma/\sqrt{3} = \tau_0 + k_{sc}(\sqrt{3}\dot{\varepsilon}^{ip})^n \quad (35)$$

The uniaxial (bulk) flow index, m , is taken equal to that of the shear flow, n , for the short fiber-reinforced fresh cementitious paste for extrusion purpose. Similar approximation was also adopted for highly viscous elasto-viscoplastic fresh ceramic pastes for extrusion purpose (Adam *et al.* 1993, Aydin *et al.* 2000). Therefore, a comparison of Eqs. (34) and (35) yields

$$\sigma_0 = \sqrt{3} \tau_0 \quad (36)$$

$$k = (\sqrt{3})^{1+m} k_{sc} \quad (37)$$

The viscoplastic strain rate in Eq. (3) is explicitly defined according to the associated flow rule by

$$\dot{\varepsilon}^{ip} = \frac{3}{2} \dot{\varepsilon}^{\bar{ip}} \frac{S}{\bar{\sigma}} \quad (38)$$

where the equivalent inelastic strain rate, $\dot{\varepsilon}^{\bar{ip}}$, is directly defined by

$$\dot{\varepsilon}^{\bar{ip}} = 0 \quad \text{for} \quad \bar{\sigma} < \sigma_0 \quad (39)$$

$$\dot{\varepsilon}^{\bar{ip}} = D_{vp} \left(\frac{\bar{\sigma} - \sigma_0}{\sigma_0} \right)^{1/m} \quad \text{for} \quad \bar{\sigma} \geq \sigma_0 \quad (40)$$

where D_{vp} and m are viscoplastic material parameters, which can be derived by rewriting Eq. (40) in the form of Eq. (34) as

$$\bar{\sigma} = \sigma_0 + \left(\frac{\sigma_0}{D_{vp}^m} \right) (\dot{\varepsilon}^{\bar{ip}})^m \quad \text{for} \quad \bar{\sigma} \geq \sigma_0 \quad (41)$$

In case of uniaxial bulk flow, $\sigma = \bar{\sigma}$ and $\dot{\varepsilon}^{ip} = \dot{\varepsilon}^{\bar{ip}}$. By comparing Eqs. (34) and (41), the two material parameters can be obtained as $D_{vp} = (\sigma_0/k)^{1/m}$ and $m = n$. Therefore, the viscoplastic material parameters, D_{vp} and m , are 0.101 s^{-1} and 0.38 , respectively, for the short fiber-reinforced fresh cementitious paste with the mix formulation shown in Table 1.

4. Results and discussion

4.1 Comparison of flow stresses from experiment and model prediction

The flow stresses of the short fiber-reinforced fresh cementitious paste, with the mix formulation shown in Table 1, at various true strains and strain rates were obtained through upsetting tests (Zhou and Li 2006). On the other hand, the flow stresses could also be predicted from the constitutive equation (Eq. (41)), which was derived mainly from results of orifice and capillary extrusion (Zhou and Li 2005b). Compared with orifice and capillary extrusion, strain and strain rate exhibited in upsetting tests were smaller. However, a comparison of flow stresses obtained from upsetting tests and from model predictions still makes sense, since the proposed constitutive model attempts to describe the constitutive behavior of the short fiber-reinforced fresh cementitious paste at the scopes of strain and strain rate experienced in various forming, including ram extrusion and upsetting,

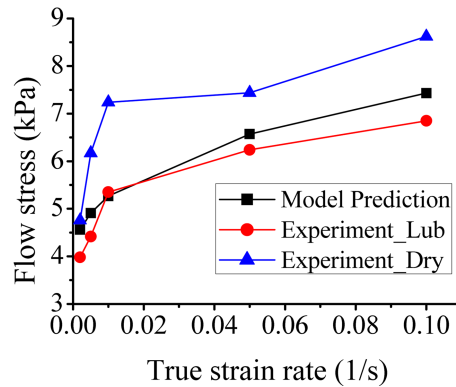


Fig. 3 Flow stress vs. strain rate for short fiber-reinforced cementitious paste

processes. It was found from upsetting tests that the flow stress tends to level off at high strain (Zhou and Li 2006). Therefore, the flow stresses of the short fiber-reinforced fresh cementitious paste at the true strain of 1.0, the maximal true strain experienced in upsetting tests, obtained from both the lubricated and the dry boundary conditions (Zhou and Li 2006), are compared with those from model predictions (see Fig. 3). The model prediction is supposed to give the true flow stress of the cementitious paste itself without the influence of any boundary friction and it should represent the lower bound of experimental results. But, in general, the results shown in Fig. 3 suggest acceptable agreement between model predictions and experimental results.

4.2 Numerical simulation of upsetting and ram extrusion processes

The increment-form computational constitutive model for the short fiber-reinforced extrudable fresh cementitious paste is implemented into a numerical procedure based on the ANSYS/LS-DYNA explicit finite element code. A series of upsetting and ram extrusion processes on the fresh cementitious paste, with the mix formulation shown in Table 1, for extrusion purpose are then simulated by the numerical procedure. Due to axisymmetry, the deformation of the deforming paste in the radial direction at the centerline of the forming process is zero. Accordingly, only a single azimuthal slice of the paste and the walls of the forming equipment are modeled in the numerical procedure. The fresh cementitious paste is modeled by Arbitrary Lagrangian-Eulerian (ALE) mesh, comprised by axisymmetric solid elements, while the forming equipment is modeled by much coarser Lagrangian mesh with the same type of elements to reduce computation time. The ALE mesh is very effective for simulating large deformation and large strain problems and it allows smoothing of a distorted mesh without requiring a complete re-meshing. Thus, it can largely avoid mesh distortion. Contact between the paste and the walls of the forming equipment is treated by a penalty approach, where the deforming paste is defined as the slave surface and the walls of the forming equipment is assigned as the master surface. A Coulomb friction criterion, with a constant friction coefficient of $\mu = 0.195$ obtained through upsetting tests (Zhou and Li 2006), is used to model boundary interaction whenever the paste contacts the walls of the forming equipment. A reduced kinematic value is used as the dynamic friction coefficient to simulate reduced boundary friction during dynamic loading.

On the other hand, upsetting and ram extrusion tests were also conducted on the short fiber-

reinforced fresh cementitious paste for extrusion purpose. The forming loads with respect to time were recorded during tests, which are then compared with the counterpart from numerical simulation. Preparation for the fresh cementitious paste for upsetting tests was the same as that for ram extrusion. The cementitious powders (cement and slag), the fibers and the Methocel powder were first mixed for 3 minutes in dry state at the lowest gauge of a Hobart mixer. Then, water (with superplasticiser) was added into the mixture and mixed with other components for another 3 minutes. Once the dry powders were sufficiently moistened, a higher speed was adjusted for 3-minutes high shear mixing. The mixing was completed when a dough-like paste was produced.

4.2.1 Numerical simulation of upsetting tests

Cylindrical specimens for upsetting tests had an initial diameter of 3 inches (76.2 mm) and initial heights of 2 inches (50.8 mm) and 3 inches (76.2 mm), respectively. They were prepared through compressing certain amount, in weight, of the fresh cementitious paste into PVC pipe moulds. The specimens were demoulded half an hour after mixing commenced and upsetting test was followed immediately after demoulding. The experimental setup and the corresponding finite element model for upsetting test are shown in Fig. 4. It should be noted that the upsetting tests referred here are different from those cited in Section 4.1, where the true strain rate was kept constant during each test. However, in the upsetting tests referred here, both the true strain and true strain rate kept increasing when the cylindrical specimens were driven by the platen with a constant velocity. These are the main differences between the two series of upsetting tests. The predicted deformation of the specimen with an initial height of 3 inches (76.2 mm) is shown in Fig. 5, which clearly indicates the typical bulge shape in upsetting process. The upsetting load-time curves, from experiment and numerical simulation, are plotted in Figs. 6(a) and 6(b) for specimens with initial height of 2 inches (50.8 mm) under the driving velocity of 0.2 mm/s and 0.5 mm/s, respectively, at the dry boundary. The difference in upsetting loads between experimental and numerical results is less than 10%.

4.2.2 Numerical simulation of ram extrusion

The experimental setup and procedure for ram extrusion were similar to those described elsewhere (Zhou and Li 2005a). An in-house extruder was employed for testing, which had a barrel with an inner diameter of 80 mm and depth of 150 mm while the die-land diameter and length were

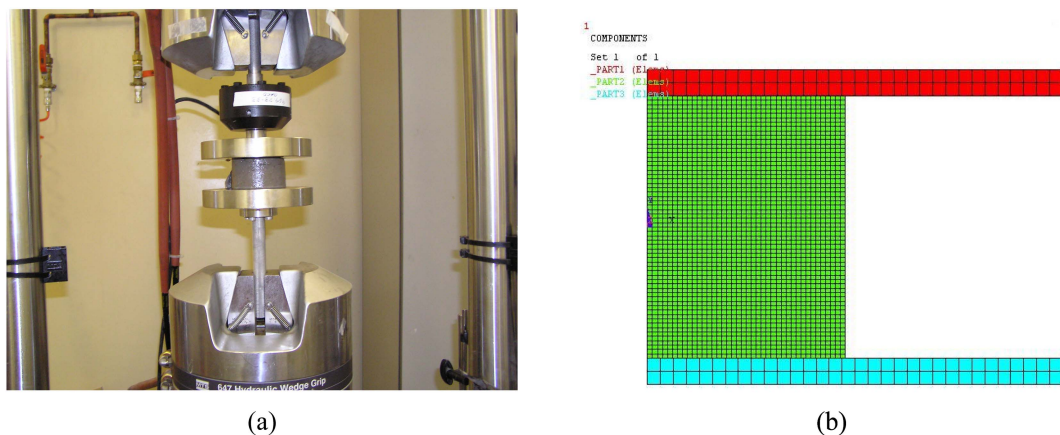


Fig. 4 (a) Experimental set-up and (b) finite element model for upsetting test

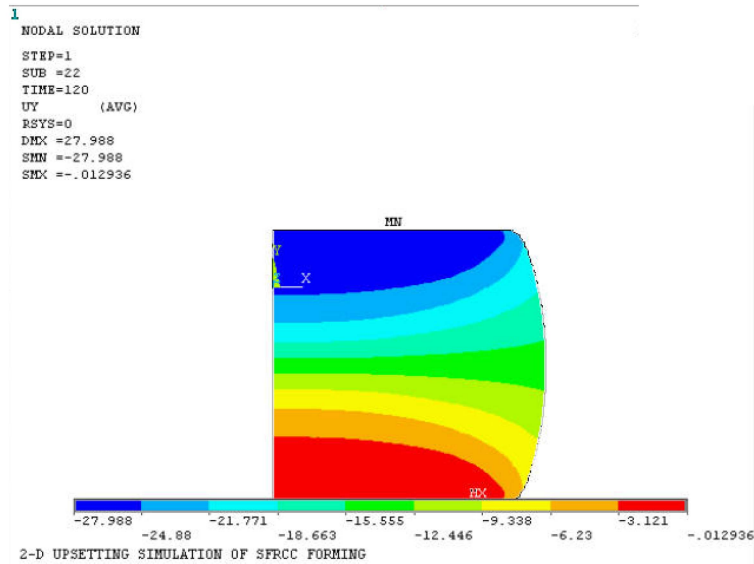


Fig. 5 Predicted deformation of a cylindrical specimen ($H = 76.2$ mm) in upsetting test

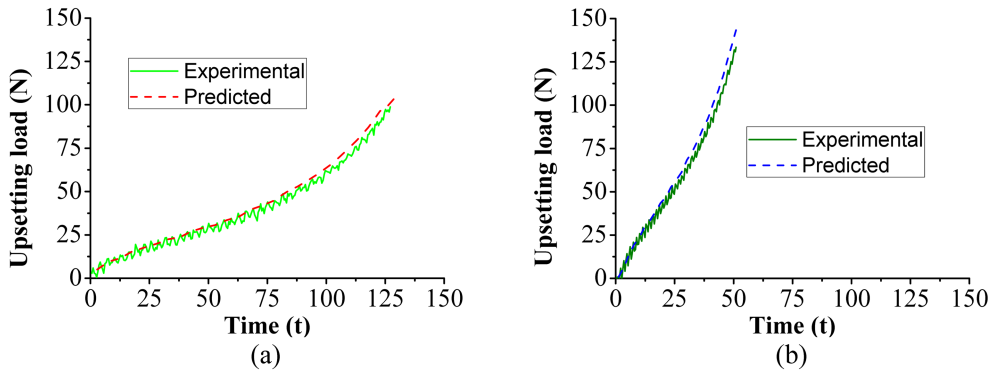


Fig. 6 Experimental and predicted upsetting load-time curves at piston driving velocity of (a) 0.2 mm/s and (b) 0.5 mm/s at dry boundary

adjustable. The ram extruder and the finite element model for ram extrusion are shown in Fig. 7. A typical flow pattern, of the fresh cementitious paste in ram extrusion, obtained from numerical simulation is presented in Fig. 8, which clearly shows the static zone at the corner of the barrel, a representative phenomenon of ram extrusion. The predicted extrusion load is plotted with respect to time to produce an extrusion load versus time curve, which is then compared with its experimental counterpart to further test the accuracy of the constitutive model for describing the elasto-viscoplastic behavior of the short fiber-reinforced extrudable fresh cementitious paste. The extrusion load-time curves, obtained through experiment and numerical simulation, are shown in Figs. 9(a) and 9(b) for two cases under a ram driving velocity of 0.1 mm/s through die-lands with diameters, D , of 12 mm and 15 mm, respectively, and die-land length-to-diameter ratios, L/D , of 0.83 and 4.79, respectively. Experimental and numerical results are in good agreement and the difference in extrusion load is less than 5% during steady state, indicating that the proposed elasto-viscoplastic



Fig. 7 (a) Experimental set-up and (b) finite element model for the ram extrusion test

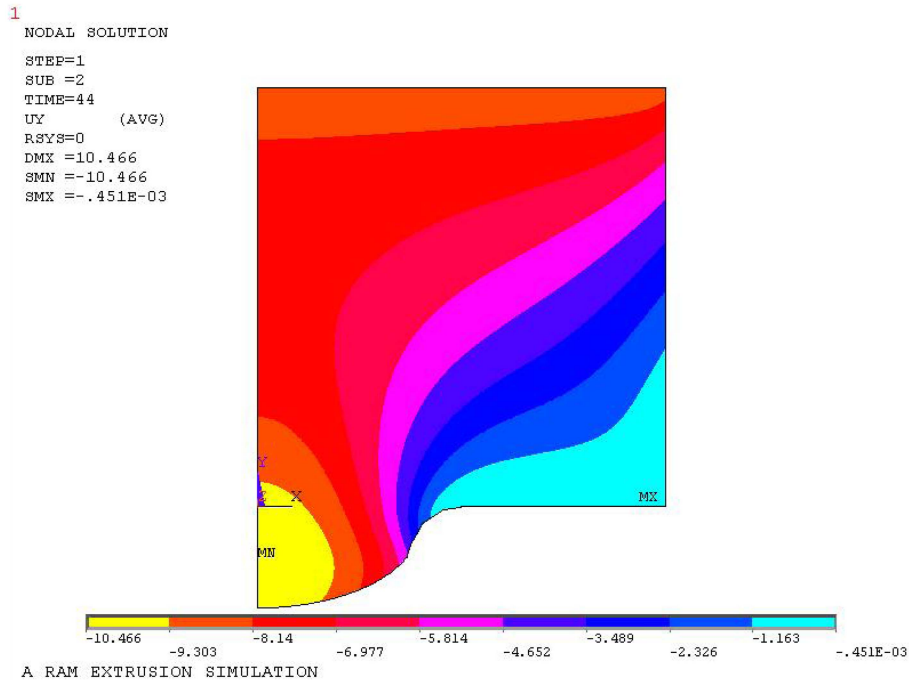


Fig. 8 Predicted typical deformation pattern of the fresh cementitious paste in ram extrusion

constitutive model can well describe the mechanical behavior of the short fiber-reinforced fresh cementitious paste for extrusion purpose.

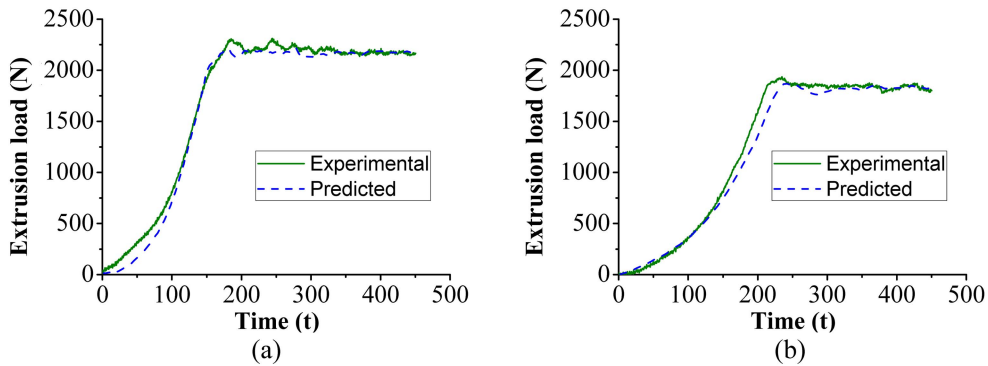


Fig. 9 Experimental and predicted extrusion load-time curves at ram driving velocity of 0.1 mm/s: (a) $D = 12$ mm and $L/D = 0.83$; (b) $D = 15$ mm and $L/D = 4.79$

5. Conclusions

In this paper, an elasto-viscoplastic constitutive model is proposed for the short fiber-reinforced fresh cementitious paste for extrusion purpose, based on the von-Mises yield criterion, the associated flow rule and the isotropic nonlinear strain rate-hardening law. The constitutive model is formulated following the consistency viscoplasticity, featured a strain rate-dependent yield function. The associated material parameters are obtained from results of material tests with simple set-ups. The flow stresses of the short fiber-reinforced fresh cementitious paste in upsetting processes are predicted by the constitutive model and compared with experimental results. The rate-form constitutive model is integrated into an incremental form and implemented into a numerical procedure based on ANSYS/LS-DYNA explicit finite element code. Various upsetting and ram extrusion processes are simulated by the numerical procedure. The predicted forming load-time data are compared with experimental results. The following conclusions can be drawn:

1. The overstress viscoplastic model is formulated by allowing the flow stress to be outside the yield surface and directly defines the plastic relaxation equations in stress space. The overstress determines the flow rule of viscoplastic strain rate. Though this kind of viscoplastic model has obvious physical meaning, it violates the general Kuhn-Tucker loading/unloading condition.

2. The consistency viscoplastic model directly defines a rate-dependent yield surface, which can expand and shrink in stress space depending on internal state variables. By doing so, the standard Kuhn-Tucker loading/unloading condition for rate-independent plasticity still remains true for rate-dependent plasticity. It has been found that the incremental formulation of the consistency viscoplastic model is similar to that of rate-independent plastic model.

3. The proposed constitutive model for the short fiber-reinforced fresh cementitious paste is based on the consistency viscoplasticity, which includes the von Mises yield criterion, the associated flow rule and the nonlinear strain rate-hardening law. For each of the physical phenomena included, one or more material constants are needed. However, all these material constants can be obtained from simple tests, including orifice, capillary extrusion and upsetting tests, without the need of numerical analysis.

4. The flow stresses of the short fiber-reinforced fresh cementitious paste, predicted by the proposed constitutive model, are in good agreement with experimental results from upsetting tests. Besides,

the predicted forming load-time curves, for upsetting and ram extrusion processes, are also in good agreement with experimental results, suggesting that the proposed computational elasto-viscoplastic constitutive model can describe the mechanical behavior of the short fiber-reinforced fresh cementitious paste in the scope of strain and strain rate exhibited in various forming processes.

Acknowledgements

The financial support from Hong Kong Research Grant Council under the grant of HKUST 6167/06E, China Ministry of Science and Technology under the grant of 2009CB632000, and Brunel Research Initiative & Enterprise Fund LBK909 (904/2009) is gratefully acknowledged. The authors would also like to thank KURARAY Co. Ltd. for providing the PVA fibers.

Reference

- Adams, M.J., Briscoe, B.J. and Kamjab, M. (1993), "The deformation and flow of highly concentrated dispersions", *Adv. Colloid Interfac.*, **44**, 143-182.
- Al-Haik, M., Vaghar, M.R., Garmestani, H. and Shahaway, M. (2001), "Viscoplastic analysis of structural polymer composites using stress relaxation and creep data", *Compos. Part B*, **32**(2), 165-170.
- Aldea, C., Marikunte, S. and Shah, S.P. (1998), "Extruded fiber reinforced cement pressure pipes", *Adv. Cement Based Mater.*, **8**(2), 47-55.
- Alfani, R., Grizzuti, N., Guerrini, G.L. and Lezzi, G. (2007), "The use of the capillary rheometer for the rheological evaluation of extrudable cement-based materials", *Rheologica Acta*, **46**(5), 703-709.
- Aydin, I., Biglari, F.R., Briscoe, B.J., Lawrence, C.J. and Adams, M.J. (2000), "Physical and numerical modelling of ram extrusion of paste materials: conical die entry case", *Comput. Mater. Sci.*, **18**(2), 141-155.
- Belytschko, T., Liu, W.K. and Moran, B. (2000), *Nonlinear finite elements for continua and structures*, John Wiley & Sons, New York.
- Chaboche, J.L. (1989), "Constitutive equations for cyclic plasticity and cyclic viscoplasticity", *Int. J. Plasticity*, **5**(3), 247-302.
- Kobayashi, S., Oh, S. and Altan, T. (1989), *Metal forming and the finite-element method*, Oxford University Press.
- Kuder, K.G. and Shah, S.P. (2007a), "Tailoring extruded HPFRCC to be nailable", *ACI Mater. J.*, **104**(5), 526-534.
- Kuder, K.G. and Shah, S.P. (2007b), "Rheology of extruded cement-based materials", *ACI Mater. J.*, **104**(3), 283-290.
- Li, Zongjin and Li, Xiangyu (2007), "Squeeze flow of viscoplastic cement-based extrudate", *J. Eng. Mech. - ASCE*, **133**(9), 1003-1008.
- Li, Z.J., Mu, B. and Chui, S.N.C. (1999), "Systematic study of properties of extrudates with incorporated metakaolin or silica fume", *ACI Mater. J.*, **96**(5), 574-579.
- Li, Z.J., Mu, B. and Chui, S.N.C. (2001), "Static and dynamic behavior of extruded sheets with short fibers", *J. Mater. Civil Eng. - ASCE*, **13**(4), 248-254.
- Li, Zongjin, Zhou, Xiangming and Shen, Bin (2004), "Fiber-cement extrudates with perlite subjected to high temperatures", *J. Mater. Civil Eng. - ASCE*, **16**(3), 221-229.
- Lof, J. (2001), "Elasto-viscoplastic FEM simulations of the aluminium flow in the bearing area for extrusion of thin-walled sections", *J. Mater. Process. Tech.*, **114**(2), 174-183.
- Lof, J. and Boogaard, A.H. Van Den (2001), "Adaptive return mapping algorithms for J_2 elasto-viscoplastic flow", *Int. J. Numer. Meth. Eng.*, **51**(11), 1283-1298.
- Ortiz, M. and Popov, E.P. (1985), "Accuracy and stability of integration algorithms for elasto-plastic constitutive relations", *Int. J. Numer. Meth. Eng.*, **21**(9), 1561-1576.
- Peled, A. and Shah, S.P. (2003), "Processing effects in cementitious composites: extrusion and casting", *J. Mater.*

- Civil Eng. - ASCE*, **15**(2), 192-199.
- Perzyna, P. (1966), *Fundamental problems in viscoplasticity*, In Kuerti, G. (Eds.), *Recent Advances in Applied Mechanics*, Academic Press, New York, **9**, 243-377.
- Ponthot, J.P. (2002), "Unified stress update algorithms for the numerical simulation of large deformation elastoplastic and elasto-viscoplastic processes", *Int. J. Plasticity*, **18**(1), 91-126.
- Qian, X.Q., Zhou, X.M., Mu, B. and Li, Z.J. (2003), "Fiber alignment and property direction dependency of FRC extrudate", *Cement Concrete Res.*, **33**(10), 1575-1581.
- Santhanam, S. (2000), "An elastic-viscoplastic constitutive model for hot-forming of aluminum alloys", *J. Mater. Sci.*, **35**(14), 3647-3654.
- Shao, Y., Marikunte, S. and Shah, S.P. (1995), "Extruded fiber-reinforced composites", *Concrete Int.*, **17**(4), 48-52.
- Shao, Y. and Shah, S.P. (1997), "Mechanical properties of PVA fiber reinforced cement composites fabricated by extrusion processing", *ACI Mater. J.*, **94**(6), 555-564.
- Shen, B., Hubler, M., Paulino, G.H. and Struble, L.J. (2008), "Functionally-graded fiber-reinforced cement composite: processing, microstructure, and properties", *Cement Concrete Compos.*, **30**(8), 663-673.
- Simo, J.C. and Hughes, T.J.R. (1998), *Computational inelasticity*, Springer-Verlag.
- Srinivasan, R., DeFord, D. and Shah, S.P. (1999), "The use of extrusion rheometry in the development of extruded fiber-reinforced cement composites", *Concrete Sci. Eng.*, **1**(1), 26-36.
- Toutou, Z., Roussel, N. and Lanos, C. (2005), "The squeeze test: a tool to identify firm cement-based material's rheological behaviour and evaluate their extrusion ability", *Cement Concrete Res.*, **35**(10), 1891-1899.
- Wang, W.M., Sluys L.J. and De Borst, R. (1997), "Viscoplasticity for instabilities due to strain softening and strain-rate softening", *Int. J. Numer. Meth. Eng.*, **40**(20), 3839-3864.
- Zhou, X. and Li, Z. (2005a), "Characterization of rheology of fresh fiber reinforced cementitious composites through ram extrusion", *Mater. Struct.*, **38**(1), 17-24.
- Zhou, Xiangming and Li, Zongjin (2005b), "Characterizing rheology of fresh short fiber reinforced cementitious composite through capillary extrusion", *J. Mater. Civil Eng. - ASCE*, **17**(1), 28-35.
- Zhou, Xiangming and Li, Zongjin (2006), "Upsetting tests of fresh cementitious composites for extrusion", *J. Eng. Mech. - ASCE*, **132**(2), 149-157.

NB